Direct Deposition and Assembly of Gold Colloidal Particles Using a Nanofountain Probe

Bin Wu, Andrea Ho, Nicolaie Moldovan, and Horacio D. Espinosa*

Department of Mechanical Engineering, Northwestern University, 2145 Sheridan Road, Evanston, Illinois 60208

Received April 24, 2007. In Final Form: June 4, 2007

We report the direct delivery and assembly of negatively charged gold colloidal particles atop positively charged amino-terminated silicon oxide surfaces using a nanofountain atomic force microscopy probe. The experimental results and fluid simulations indicate that the flow of nanoparticles is confined to the core tip region of the probe. This leads to the assembly of high-resolution submicron patterns (200 nm) on the substrate with feature sizes dependent on the tip−substrate contact time. A diffusion mechanism for the patterning is proposed and discussed.

Introduction

Significant advances have been made in manipulating, delivering, and assembling a wide range of nanomaterials in predefined architectures and patterns. These materials include organic molecules, nanoparticles, biological molecules, and small liquid droplets containing active components. The realization of these architectures has depended largely on the development of nanolithographic techniques such as microcontact printing,[1] dip pen nanolithography (DPN),[2] microfluidic network printing,[3−5] inkjet printing,[6] or fountain pen based printing.[7−11] In general, these methods rely on the transfer of molecules to chemically functionalized surfaces. The molecules are chemo-physically adsorbed on an ink delivery tip or mold in a dry state or carried by a fluid in a microfluidic device. While contact is made between the apex of the device and a surface, the molecules are adsorbed onto the surface. The size of the deposited feature can be controlled by the contact time and the probe tip geometry. For example, the DPN technique has achieved a resolution of a few tens of nanometers in the case of molecular patterning. However, direct writing with nanoparticles by DPN has proven to be challenging, most likely due to inefficient particle coating of the atomic force microscopy (AFM) tip or rapid loss of particle mobility during solvent evaporation. Thus far, there have been few successful attempts to directly deposit nanoparticles by DPN. A previously reported approach was based on a modified inking method, which allows Au nanoparticles to be coated on the AFM tip in a liquid state.[12,13] However, the throughput and controllability of the nanoparticle deposition are still poor. Indeed, direct nanoparticle pattering is important for many applications such as the fabrication of nanoscale electronic circuits and waveguides.[14] Many challenges remain in assembling and positioning nanoparticles in desired locations to construct complex, functional structures.

Controlled deposition and patterning of Au nanoparticles have been achieved by top-down, bottom-up, or a combination of both methods using template-directed assembly[15] or evaporation-induced assembly.[16,17] However, direct write methods provide better control over resultant patterns and simplify the process of making functional structures. Nanofountain probe (NFP) patterning is a promising direct write approach capable of delivering liquids to a surface. In the past, microfluidic components such as reservoirs, microchannels, and small apertures or slots have been used to control the delivery of ink solutions. However, the previously reported microfluidic tools suffer from low deposition resolution and poor control of the liquid spreading on the substrate. Recently, following the development of the first and second generations of the NFP in our lab,[18−20] a third generation of the NFP was fabricated. Modifications included fabrication on SOI wafers, improved channel sealing, deeper channels to allow the delivery of larger particles and more robust fabrication processes leading to enhanced yield. Here we describe the direct patterning of Au nanoparticles using the third generation of nanofountain probes, which integrate a volcano-shaped tip, microfluidic channels along 24 cantilevers, and 4 reservoirs all in one chip. Delivered Au nanoparticles were electrostatically bound to amino-terminated oxidized silicon substrates in a reliable and reproducible fashion.

* To whom correspondence should be addressed. E-mail: espinosa@northwestern.edu.

(1) Xia, Y.; Rogers, J. A.; Paul, K.; Whitesides, G. M. *Chem. Rev.* **1999**, *99*, 1823.
(2) Piner, R. D.; Zhu, J.; Xu, F.; Hong, S.; Mirkin, C. A. *Science* **1999**, *283*, 661.
(3) Delamarche, E.; Bernard, A.; Schmid, H.; Michel, B.; Biebuyck, H. *Science* **1997**, *276*, 779.
(4) Kenis, P. J. A.; Ismagilov, R. F.; Whitesides, G. M. *Science* **1999**, *285*, 83.
(5) Chiu, D. T.; Jeon, N. L.; Huang, R.; Kane, R. S.; Wargo, C. J.; Choi, I. S.; Ingber, D. E.; Whitesides, G. M. *Proc. Natl. Acad. Sci.* **2000**, *97*, 2408.
(6) Cuk, T.; Troian, S. M.; Hong, C. M.; Wagner, S. *Appl. Phys. Lett.* **2000**, *77*, 2063.
(7) Lewis, A.; Kheifetz, Y.; Shambrodt, E.; Radko, A.; Khatchatryan, E.; Sukenik, C. *Appl. Phys. Lett.* **1999**, *75*, 2689.
(8) Deladi, S.; Tas, N. R.; Berenschot, J. W.; Krijnen, G. J. M.; De Boer, M. J.; De Boer, J. H.; Peter, M.; Elwenspoek, M. C. *Appl. Phys. Lett.* **2004**, *85*, 5361.
(9) Dockendorf, C. P. R.; Choi, T. Y.; Poulikakos, D.; Stemmer, A. *Appl. Phys. Lett.* **2006**, *88*, 131903−1.
(10) Meister, A.; Liley, M.; Brugger, J.; Pugin, R.; Heinzelmann, H. *Appl. Phys. Lett.* **2004**, *85*, 6260.
(11) Meister, A.; Jeney, S.; Liley, M.; Akiyama, T.; Staufer, U.; de Rooij, N. F.; Heinzelmann, H. *Microelectronic Eng.* **2003**, *67*−*68*, 644.
(12) Ali, M. B.; Ondarcuhu, T.; Brust, M.; Joachim, C. *Langmuir* **2002**, *18*, 872.
(13) Prime, D.; Paul, S.; Pearson, C.; Green, M.; Petty, M. C. *Mater. Sci. Eng. C* **2005**, *25*, 33.
(14) Zhang, X. P.; Sun, B. Q.; Friend, R. H.; Guo, H. C.; Nau, D.; Giessen, H. *Nano Lett.* **2006**, *6*, 651.
(15) Cui, Y.; Bjork, M. T.; Liddle, J. A.; Sonnichsen, C.; Boussert, B.; Alivisatos, A. P. *Nano Lett.* **2004**, *4*, 1093.
(16) Bigioni, T. P.; Lin, X. M.; Nguyen, T. T.; Corwin, E. I.; Witten, T. A.; Jaeger, H. M. *Nat. Mater.* **2006**, *5*, 265.
(17) Sheu, J. T.; Wu, C. H.; Chao, T. S. *Jpn. J. Appl. Phys.* **2006**, *45*, 3693.
(18) Kim, K. H.; Moldovan, N.; Espinosa, H. D. *Small* **2005**, *1*, 632.
(19) Moldovan, N.; Kim, K. H.; Espinosa, H. D. *J. Micromech. Microeng.* **2006**, *16*, 1935.
(20) Moldovan, N.; Kim, K. H.; Espinosa, H. D. *J. Microelectromech. Syst.* **2006**, *15*, 204−213.

10.1021/la7011952 CCC: $37.00
Published on Web 07/24/2007

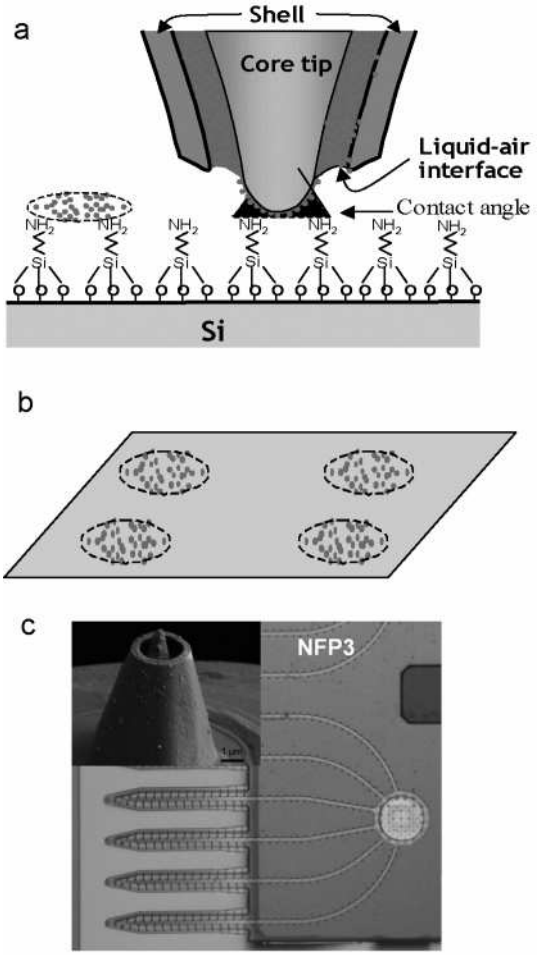

Figure 1. (a) Schematic of Au nanoparticle delivery by the nanofountain probe; (b) Schematic of dot pattern containing nanoparticles. (c) Optical image of NFP cantilevers; inset: aperture of probe tip.

Materials and Methods

The colloidal Au solution (Ted Pella, Inc.) was a water solution containing gold colloids with an average particle diameter of 15 nm. The particles were capped with citrate ions, rendering them negatively charged. Prior to use, Au sol was concentrated up to 100 times by centrifugation, resulting in a concentration of 1.4×10^{14} particles/mL.

Figure 1 illustrates the scheme for simultaneous Au nanoparticle deposition and assembly. The aqueous gold colloidal solution was transported from the NFP chip reservoir to the tip apex by capillarity. Prior to patterning, the oxidized silicon wafer substrate was functionalized with a 3-aminopropytriethoxysilane (APTES) monolayer formed by soaking the substrate in an APTES solution in ethanol (0.1% v/v) for 1 h, then rinsing successively in ethanol and water, and drying with high purity nitrogen. The substrate was then baked at 120 °C for 1−2 h to complete the Si−O bond formation. The affinity of the amino groups to gold is driven by strong electrostatic interactions, immobilizing the Au particles on the silane-coupler treated substrate.[21] Sol delivery by the NFP allowed Au nanoparticles to be immobilized on the substrate in one step.

Aqueous gold sol (~1 μL) was fed into two reservoirs of the NFP using a micropipette. The chip was immediately mounted on an AFM instrument (Veeco Dimension 3100). All experiments were performed at a relative humidity of 50−65%, at room temperature. Patterned arrays were produced by custom scripts developed with Nanoscript software.[22] The NFP was able to pattern for more than

(21) Sato, T.; Hasko, D. G.; Ahmed, H. *J. Vac. Sci. Technol. B* **1997**, *15* (1), 45.

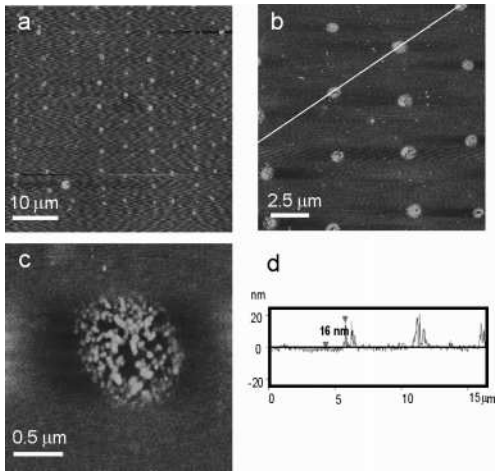

Figure 2. Tapping mode AFM images of patterned Au nanoparticles (a−c) and the height profile along the line in image b (d).

40 min, which is consistent with the evaporation time of water-based liquids within the channels, as observed by optical microscopy. No wear of the nitride tip was noticeable after the working period, which is consistent with the relatively short path described by the tip in friction mode, although a large range of contact forces were tested. This differs from the scanning of large surfaces in imaging mode, where wear work is caused by long paths and small contact forces. Occasionally, the NFP tips became clogged with nanoparticles, thereby precluding further deposition. However, chemical cleaning procedures such as with piranha solution (7:3 H_2SO_4:H_2O_2 by volume) were capable of clearing the probes, making the NFPs reusable.

Results and Discussion

Dot patterns were produced with different NFP-to-substrate contact times, to investigate the Au nanoparticle diffusion and the repeatability of the writing process. After full evaporation of the solvent, the patterned area was imaged by tapping mode AFM using commercial Si cantilevers. Arrays of 600−700 nm diameter dots of Au particles spaced 4 μm apart were deposited on a substrate with a contact time of 2 s as shown in Figure 2. The deviation in dot position is due to the scanning piezo tube hysteresis, as the employed AFM did not possess closed-loop feedback. Immediately after patterning, the features were as high as 180 nm, which is much greater than the height of one monolayer of Au particles (see the Supporting Information). After thoroughly rinsing the sample with DI water (Figure 2a−c), the dot arrays remained on the surface, and the average height of the dots was dramatically reduced to about 15−20 nm, which is in good agreement with the nanoparticle diameter measured from AFM and scanning electron microscopy (SEM) images of individual particles. Well-resolved individual particles can be seen in the magnified images in Figure 2b,c. A 2 s contact time resulted in a significant delivery of Au particles to the substrate and the subsequent assembly of a particle multilayer. The particles and the nonvolatile residue present in the Au sol (sodium citrate) were responsible for the initial height profile. Subsequent rinsing removed the nonimmobilized particles and residues, leaving behind a well-defined particle monolayer pattern. The experiments also show that it is possible to form dot arrays consisting of two layers of Au particles, confirmed by an average height of 20−30 nm (see the Supporting Information).

Direct optical microscopy observation provided further evidence of Au particle deposition. The dot arrays exhibited the same characteristic pink color as that of a large area of gold

(22) Veeco Metrology, Inc., Santa Barbara, CA.

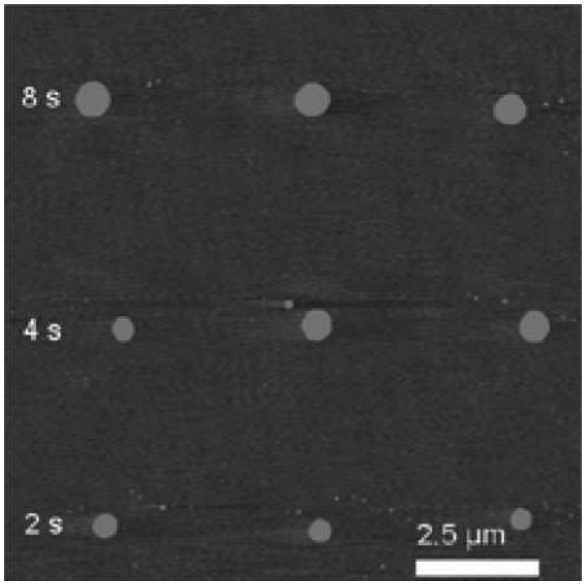

Figure 3. Tapping mode AFM image of nanoparticle spots patterned with varying tip-substrate contact times.

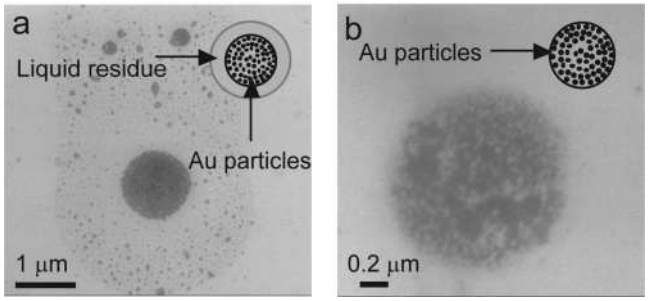

Figure 4. SEM images of patterned substrates (a) prior to rinsing in DI water, delineating the liquid residue area and central region containing Au nanoparticles and (b) after rinsing, showing a monolayer of Au nanoparticles. Schematics are shown in the insets.

particle film assembled on the same substrate. The same NFP chip could be employed in multiple instances, even after complete evaporation of the solvent, by refilling it with Au nanoparticle sol. The patterns produced were generally very repeatable in size and shape. A dramatic reduction in dot size was observed immediately before the patterning ceased, perhaps due to the rapid loss of solvent as it completely evaporated away. By contrast, when different NFP chips were employed, a contact time of 2 s resulted in a range of spot diameters. Our investigation showed that the spot size primarily depends on three factors: nanofountain probe tip dimensions, wetting characteristics, and evaporation rate. We are currently investigating the effect of these parameters on the nanoparticle deposition mechanism and resolution. The effect of contact force was examined by changing the feedback setpoint within the detectable range of the photodiode on the AFM. However, no appreciable dependence of the spot size on the applied normal force was observed.

Both the diameter and the height of Au dots could be controlled by varying the tip−substrate contact time as shown in Figure 3. SEM images of patterned substrates (Figure 4a) before rinsing with DI water revealed an area of nonvolatile residue left on the substrate after solvent evaporation. After rinsing the substrate (Figure 4b), this residue was completely removed. This nonvolatile, water soluble residue is likely sodium citrate, as citrate was the only substance other than gold nanoparticles present in the patterned solution. The residue area increased very little for varying tip−substrate contact times, whereas the lateral dimensions and height of the central Au particle area increased with increasing tip−substrate contact times. Scaling analysis of the patterns revealed that the nanoparticle spot diameter in μm depended on the contact time in seconds as $D \propto 0.47t^{0.183}$ (Figure 5), whereas the extent of the residue depended on time as $D \propto 2.9t^{0.091}$. The generic power law dependence of the dot diameter on time $D \propto at^{\nu}$ stems from a surface diffusion model advanced by Jang et al.,[23] where $\nu = 0.5$ and a depends on the ratio of the surface diffusion coefficient to the ink deposition rate. The power law relation was later extended to characterize other types of dot formation mechanisms, whereas the deviation of the experimentally determined ν exponent from the surface diffusion value (0.5) indicates the deviation from the surface diffusion model. Two values for the exponent can be determined: ν_m by considering the diameter of the circle circumscribing the dot or ν_a by considering the diameter of the circle of equal area with the dot.[24] ν_a typically remains close to 0.5, whereas ν_m exhibits larger deviations. The results reported here for the exponent correspond to ν_m. Although more data points would be needed to determine ν more accurately, the current analysis strongly indicates that the dot growth is substantially slower than in a surface diffusion-driven model, both for the nanoparticle dots and the surrounding water-soluble spots.

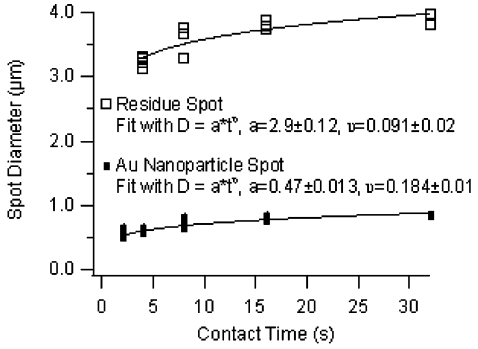

Figure 5. Spot diameter as a function of tip-substrate contact time for gold nanoparticles and soluble residues.

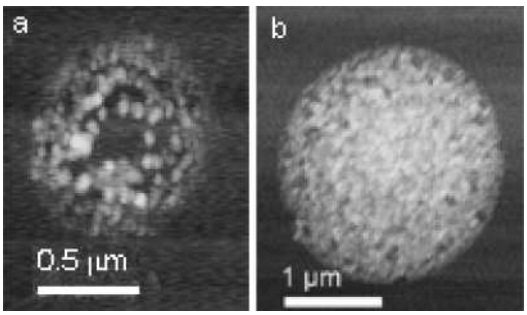

Figure 6. Tapping mode AFM images of a patterned (a) hollow dot and (b) filled dot.

The proposed deposition mechanism involves the formation of a thermodynamically stable liquid−air interface by capillary action, followed by the spreading of the liquid on the substrate upon contact. Given the fact that deposited Au particles do not follow the spreading of the liquid, the particle distribution in the meniscus is not homogeneous. This is consistent with the occasional formation of hollow circular dots (Figure 6a) instead of the usual completely filled dots (Figure 6b). This phenomenon may be explained by an annular diffusion model in which solute

(23) Jang, J.; Hong, S. H.; Schatz, G. C.; Ratner, M. A. *J. Chem. Phys.* **2001**, *115*, 2721.
(24) Manandhar, P.; Jang, J.; Schatz, G. C.; Ratner, M. A.; Hong, S. *Phys. Rev. Lett.* **2003**, *90*, 115505.

transport is slower than the condensation leading to the formation of the meniscus, and molecules are transported at the air−water interface of the meniscus.[25] Furthermore, previous studies have shown that suspensions of nanometer-sized particles (nanofluids) spreading on a surface develop a wedge-shaped film at the front that is a three-phase contact region.[26] Colloidal particles tend to accumulate in this region in an ordered, crystal-like structure that is denser than the disordered, fluid-like bulk region. Therefore, high-density deposition of Au particles within dots is possible whenever Au particles accumulated at the triple phase contact line directly contact the amino-terminated silicon surface. Dynamic growth of the nanoparticle patterns is then driven by concentration gradient induced particle diffusion on the substrate in both lateral and vertical directions, and the resulting patterns are then balanced by the competition between repulsive forces between negatively charged particles, attractive interactions between particles and the substrate, and lateral diffusion.

To investigate the effect of wetting, controlled experiments were conducted on different substrates providing a range of contact angles between the nanoparticle ink and the substrate. Generally, dot sizes on APTES/SiO_2, Au, and mercaptohexadecanoic acid (MHA)-coated Au substrates increased with decreasing contact angles. However, these substrates could not immobilize Au particles; rinsing with DI water removed all of the deposited particles. Furthermore, newly prepared substrates were required to obtain reproducible results. In general, no nanoparticle patterns could be observed on substrates stored in air for more than 10 days, due to an increase in the contact angle of the nanoparticle solution on the substrate.

Like nanopipettes[27,28] and surface patterning tools[29] (SPTs), the NFP delivers a sample solution through a microchannel. However, the solution delivered through the NFP microchannel stops at the ring shaped aperture of the volcano tip to form a liquid−air interface. Subsequently, molecules move out of the interface to diffuse along the surface of the inner tip and then to the surface. Previous numerical simulations of fluid transport through the NFP performed using commercial software (CFD-ACE+, CFDRC) indicated that liquid ink can flow through the microchannels due to the capillary force resulting from the small channel dimensions. These simulations demonstrated that the equilibrium liquid−air interface is determined by the geometry of the device and the contact angles of the liquid ink on the solid wall surfaces. In some cases, the liquid could leak outside the channel, and the formation of vapor bubbles due to cavitation was predicted and experimentally observed.[30] More recently, a two-dimensional axi-symmetric model was simulated in Fluent (ANSYS, Inc.), based on the geometry of the third generation nanofountain probe, which was used in the experiments reported here. A core with an apex radius of 250 nm protruding 625 nm from the outer shell was modeled. Experimentally measured values of the contact angles of the nanoparticle solution on the NFP material and on the substrate were used. Moreover, simulations were performed for the fountain probe in contact with the substrate, and the capillary flow was computed. For the Si_3N_4 NFP, the simulations confirmed that a stable fluid−air interface exists, and the meniscus shape is as depicted in Figure 1 with no bubble formation. The liquid is confined to the core tip region during fluid delivery.

Conclusion

The direct deposition of Au nanoparticles in solution by means of the nanofountain probe patterning method was demonstrated. The experimental results and fluid simulations indicate that the flow and deposition of nanoparticles is confined to the core tip region of the NFP, which leads to the assembly of high-resolution submicron patterns with feature sizes as small as 200 nm. The study also reveals that contact angle, time, tip material, and buffer chemistry control the shape of the liquid meniscus and the deposition rate. Thus, the NFP allows unprecedented spatial control in the direct deposition of Au nanoparticles.

Acknowledgment. This work was supported primarily by the Nanoscale Science and Engineering Initiative of the National Science Foundation under NSF Award Number EEC−0118025. The authors acknowledge the Microfabrication Applications Laboratory (MAL) of the University of Illinois at Chicago, the Cornell NanoScale Science & Technology Facility (CNF) of Cornell University, the Materials Processing and Crystal Growth Facility (MPCGF) of Northwestern University, and Northwestern University Atomic- and Nanoscale Characterization Experimental Center (NUANCE). B.W. acknowledges useful discussions with Raymond Sanedrin and his assistance with nanoparticle centrifugation.

Supporting Information Available: Figures indicating that gold nanoparticles deposited by the nanofountain probe can form bilayers. This information is available free of charge via the Internet at http://pubs.acs.org.

LA7011952

(25) Nafday, O. A.; Vaughn, M. W.; Weeks, B. L. *J. Chem. Phys.* **2006**, *125*, 144703.
(26) Wasan, D. T.; Nikolov, A. D. *Nature* **2003**, *423*, 156.
(27) Bruckbauer, A.; Ying, L. M.; Rothery, A. M.; Zhou, D. J.; Shevchuk, A. I.; Abell, C.; Korchev, Y. E.; Klenerman, D. *J. Am. Chem. Soc.* **2002**, *124*, 8810.
(28) Bruckbauer, A.; Zhou, D. J.; Ying, L. M.; Abell, C.; Klenerman, D. *Nano Lett.* **2002**, *4*, 1859.
(29) Xu, J.; Lynch, M.; Huff, J. L.; Mosher, C.; Vengasandra, S,; Ding, G.; Henderson, E. *Biomed. Microdevices* **2004**, *6*, 117.
(30) Kim, K.-H.; Ke, C.; Moldovan, N.; Espinosa, H.D. In *Proceedings of the 4th International Symposium on MEMS and Nanotechnology*; Charlotte, North Carolina, 2003; Society for Experimental Mechanics: Bethel, CT.